scientific reports

Check for updates

OPEN

Comparative analysis of the postadmission and antemortem oropharyngeal and rectal swab microbiota of ICU patients

Annamaria Petrilla[1,8], Peter Nemeth[1,8], Peter Fauszt[2], Anna Szilagyi-Racz[2], Maja Mikolas[2], Emese Szilagyi-Tolnai[2], Peter David[2], Aniko Stagel[3], Ferenc Gal[2], Kristof Gal[4], Reka Sohajda[3], Trinh Pham[5], Laszlo Stundl[6], Sandor Biro[7], Judit Remenyik[2] & Melinda Paholcsek[2]✉

Shotgun metabarcoding was conducted to examine the microbiota in a total of 48 samples from 12 critically ill patients, analyzing samples from both the oropharynx and rectum. We aimed to compare their postadmission microbiota, characterized as moderately dysbiotic, with the severely dysbiotic antemortem microbiota associated with patients' deaths. We found that, compared with postadmission samples, patient antemortem swab samples presented moderate but not significantly decreased diversity indices. The antemortem oropharyngeal samples presented an increase in biofilm-forming bacteria, including *Streptococcus oralis*, methicillin-resistant *Staphylococcus aureus* (MRSA), and *Enterococcus faecalis*. Although the septic shock rate was 67%, no significant differences were detected in the potential pathogen ratios when the microbiota was analyzed. A notable strain-sharing rate between the oropharynx and intestine was noted. By comparing postadmission and antemortem samples, microbial biomarkers of severe dysbiosis were pinpointed through the analysis of differentially abundant and uniquely emerging species in both oropharyngeal and rectal swabs. Demonstrating strong interconnectivity along the oral-intestinal axis, these biomarkers could serve as indicators of the progression of dysbiosis. Furthermore, the microbial networks of the oropharyngeal microbiota in deceased patients presented the lowest modularity, suggesting a vulnerable community structure. Our data also highlight the critical importance of introducing treatments aimed at enhancing the resilience of the oral cavity microbiome, thereby contributing to better patient outcomes.

Multiple microbiomes are associated with the human body, among which the intestinal and oral cavity microbiota are significant, and play crucial roles in the physiological processes of the human host[1,2]. Intensive care unit (ICU) patients battling severe underlying illnesses require multiple therapeutic interventions. Antibiotic administration, altered nutritional support, and the physiological stress response to critical illness profoundly influence the delicate balance of their microbiota[3–5].

It is becoming increasingly evident that microbial communities are connected through physical and metabolic interactions, such as co-adhesion and the exchange of signaling molecules and metabolites[6,7]. Polymicrobial synergy arises from interactions like nutrient sharing and cooperative substrate degradation[8,9]. However, in dysbiotic environments, this synergy is often disrupted[10]. Disrupted microbial communities in the oropharynx can lead to systemic conditions characterized by the breakdown of innate barriers, immune dysregulation, and heightened pro-inflammatory signaling, particularly within the intestine[11–13]. The compromised physical defense barriers have been linked to increased susceptibility to infections, delayed recovery, and extended hospital stays[14,15].

[1]Department of Anaesthesiology and Intensive Care, Vas County Markusovszky Teaching Hospital, Szombathely, Hungary. [2]Faculty of Agricultural and Food Sciences and Environmental Management, Complex Systems and Microbiome-innovations Centre, University of Debrecen, Debrecen, Hungary. [3]Hungarian National Blood Transfusion Service Nucleic Acid Testing Laboratory, Budapest, Hungary. [4]Department of Oncoradiology, University of Debrecen Clinical Centre, Debrecen, Hungary. [5]Turku Bioscience Centre, University of Turku and Abo Akademi University, 20520 Turku, Finland. [6]Faculty of Agricultural and Food Sciences and Environmental Management, University of Debrecen, Debrecen, Hungary. [7]Department of Human Genetics, Faculty of Medicine, University of Debrecen, Debrecen, Hungary. [8]These authors contributed equally: Annamaria Petrilla and Peter Nemeth. ✉email: paholcsek.melinda@agr.unideb.hu

Symbiotic microbiota offers protection against colonization by external pathogens. However, in critical illness, the increased stress caused by various treatments and interventions can disrupt the native intestinal microbiota, and can lead to the overgrowth of potentially harmful pathogens[16,17]. The progression of infections accelerates due to dysbiotic microbiomes leading to different levels of disease severity characterized by distinct microbial changes[18,19]. Anaerobic bacteria play a significant role in the microbiome of patients with weakened immune systems. By providing colonization resistance anaerobic bacteria in the gut help maintain balance and resist colonization by pathogenic organisms[20,21]. These gut anaerobes protect against pneumonia, organ failure, and mortality[22].

Identifying key species that may act as early indicators of worsening clinical conditions is of paramount importance.

Both in diagnostics and therapeutic interventions, increasing focus is being placed on the gut microbiota, as it represents one of the most abundant and metabolically active microbial ecosystems. However, studying these microbiomes in critically ill patients presents significant challenges. Oropharyngeal swab samples, being more easily accessible, could provide specific biomarkers to predict microbial changes in the gastrointestinal tract that characterize severely dysbiotic microbiomes.

In this study, we aimed to compare the ICU patients' postadmission microbiotas, identified as moderately dysbiotic, with the severely dysbiotic antemortem microbiotas linked to their deaths. Another objective of our research was to clarify the relationship between the oropharyngeal and rectal microbiomes in ICU patients. By tracking microbial shifts from the time of ICU admission to the last 1–2 days before death, we aimed to uncover significant microbial ecosystem changes that occur as patients' conditions worsen.

Specifically, we focused on changes in microbial diversity, composition, and the balance of Gram-positive and Gram-negative bacteria, eukaryotes, anaerobes, and biofilm-forming pathogens.

Additionally, we sought to identify microbial biomarker species that could serve as indicators of the progression of dysbiosis. For these, we sought to explore the core microbiota shared between the oropharynx and rectum, identifying key species that showed strong correlations between these anatomical sites.

Finally, we aimed to compare the resilience of moderately dysbiotic microbial communities to those experiencing more severely distorted communities in ICU patients, focusing on shifts in community densities and modularity. These metrics are key indicators of how dysbiotic microbial communities adapt and attempt to restore ecological balance[23].

Results

Description of study participants

Our follow-up study involved 69 recruited intensive care unit (ICU) patients admitted between February 13 and June 22, 2023, with oropharyngeal and rectal swab samples collected every three days. Inclusion criteria required adult patients admitted to the ICU ward, with an anticipated stay of at least 48 h, who eventually died there. Based on these our study cohort involved 12 patients (8 males, 4 females) with a mean age of 68.67 ± 10.85 years and had a median hospital stay of 11 days (range, 5–29 days) (Fig. 1). Their medical history revealed a range of preexisting conditions, with 7 patients (58%) having cardiovascular and chronic lung diseases, and 11 patients (92%) suffering from hypertension (Supplementary Table 1). Additionally, complications such as cirrhosis and other comorbidities were noted. The majority of the patients, (10 out of 12, 83%), were admitted for pulmonary issues, including COPD and pneumonia. Sepsis was also a common reason for admission (75%), leading to septic shock in 8 patients (67%) and ultimately being the cause of death. Three patients (25%) also experienced acute heart failure. Other reasons for admission included various medical and surgical conditions, such as peritonitis or drug overdose. In five patients, respiratory infections were diagnosed during their hospital stay, with four cases (patient Nos. 4, 5, 6, and 11) likely associated with ventilator use and one (patient No. 12) probably associated with health care. Disease severity, assessed by the APACHE II score (mean score: 19.5) and SOFA score (range: 2–17), varied across the cohort. Treatment during the hospital stay included invasive or noninvasive mechanical ventilation (12, 100%), enteral (12, 100%) and parenteral (4, 33%) nutrition to meet nutritional needs and empirical or targeted antibiotics, with 10 out of 12 patients (83%) receiving antibiotics upon intensive care unit (ICU) admission.

Description of the shotgun sequencing results

Shotgun metagenomic sequencing was carried out on the Illumina NovaSeq platform (Illumina, USA). A total of 39,289,881 ± 11,782,090 average reads per sample were obtained. The average number of reads of *Archaea* was 69,732 ± 156,227, *Bacteria* was 23,728,886 ± 16,769,257, *Eukaryota* was 8,028,620 ± 7,061,493 and *Virus* was 206,922 ± 52,709 reads per sample.

A remarkable shift in eukaryotes was observed in the severely dysbiotic microbiota of patients' oropharyngeal samples

Changes in bacterial proportions and Gram ratios in oropharyngeal (OS) and rectal (RS) swab samples were analyzed in patients admitted to the ICU (Fig. 2). The results showed that the proportion of *bacteria* decreased, though not significantly, in both oropharyngeal swab and rectal swab samples when comparing antemortem (AM) to postadmission (PA) samples. Specifically, in OS samples, the proportion dropped from 95.5 to 92.76%, while in RS samples, it decreased from 97.62 to 95.75% (Fig. 2a). The decrease in the bacterial proportion was 2.74% ± 0.077 for the OS samples and 1.87% ± 0.091 for the RS samples. In the OS samples, the ratio of gram-positive bacteria increased (PA: 60.3% ± 26.0 vs. AM: 72.3% ± 27.0), whereas in the RS samples, the ratio changed only moderately (PA: 59.6% ± 13.0 vs. AM: 54.6% ± 20.1). Interestingly, we found that the proportion of eukaryotes increased in oropharyngeal swab samples (PA: 3.03% ±0.05 vs. AM: 6.81% ± 0.096). In oropharyngeal samples, the percentage of eukaryotes in antemortem samples more than doubled (3.03-6.81%)

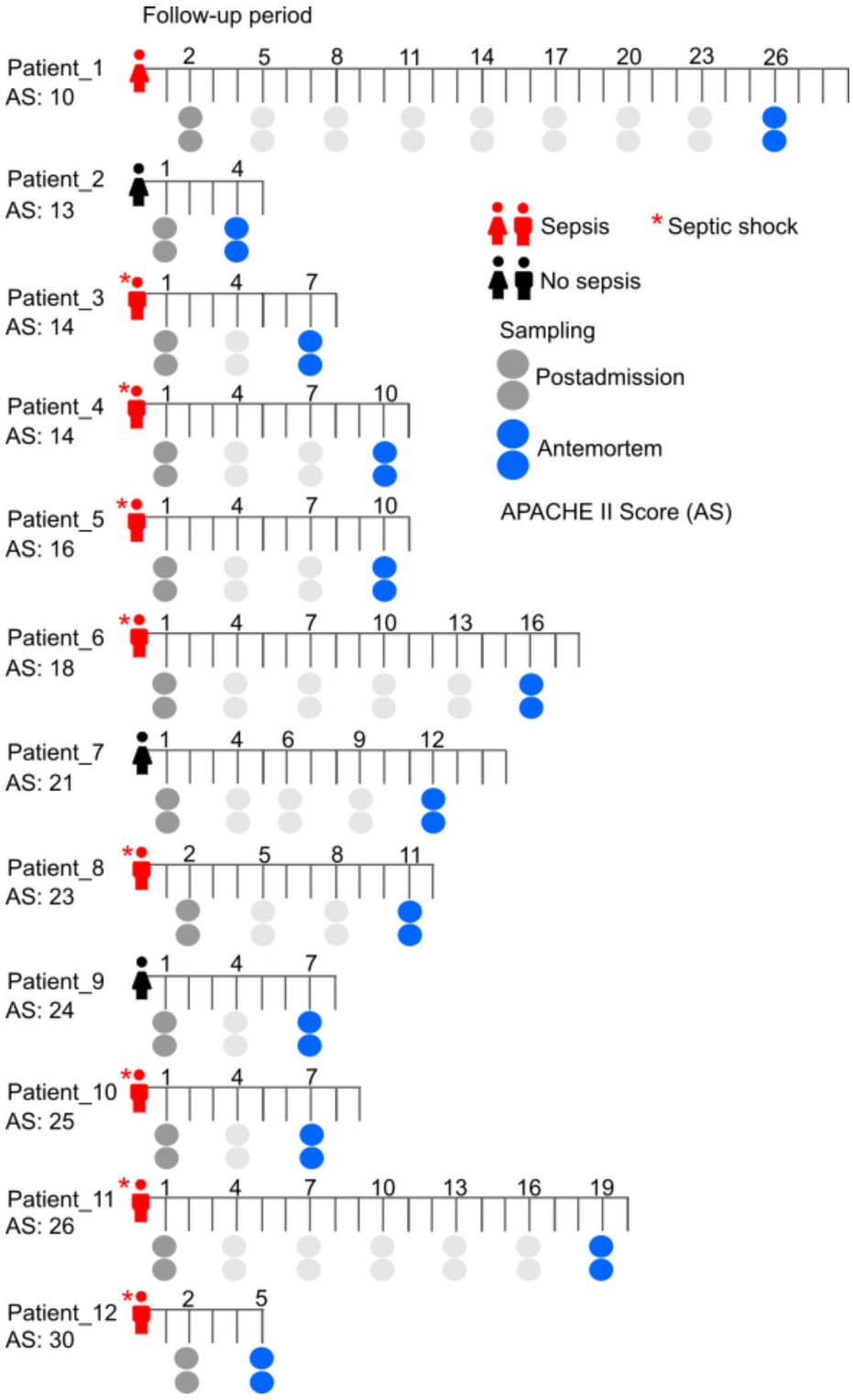

Fig. 1. Overview of the study cohort. The figure illustrates the 12 patients included in the study, indicating their gender, APACHE II score, and a timeline that shows the number of days they stayed in the intensive care unit (ICU) until their death. Additionally, it highlights the intervals at which oropharyngeal and rectal swabs were simultaneously collected. A distinction is made between postadmission and antemortem samples to show how samples were taken throughout their ICU stay and closer to the time of death.

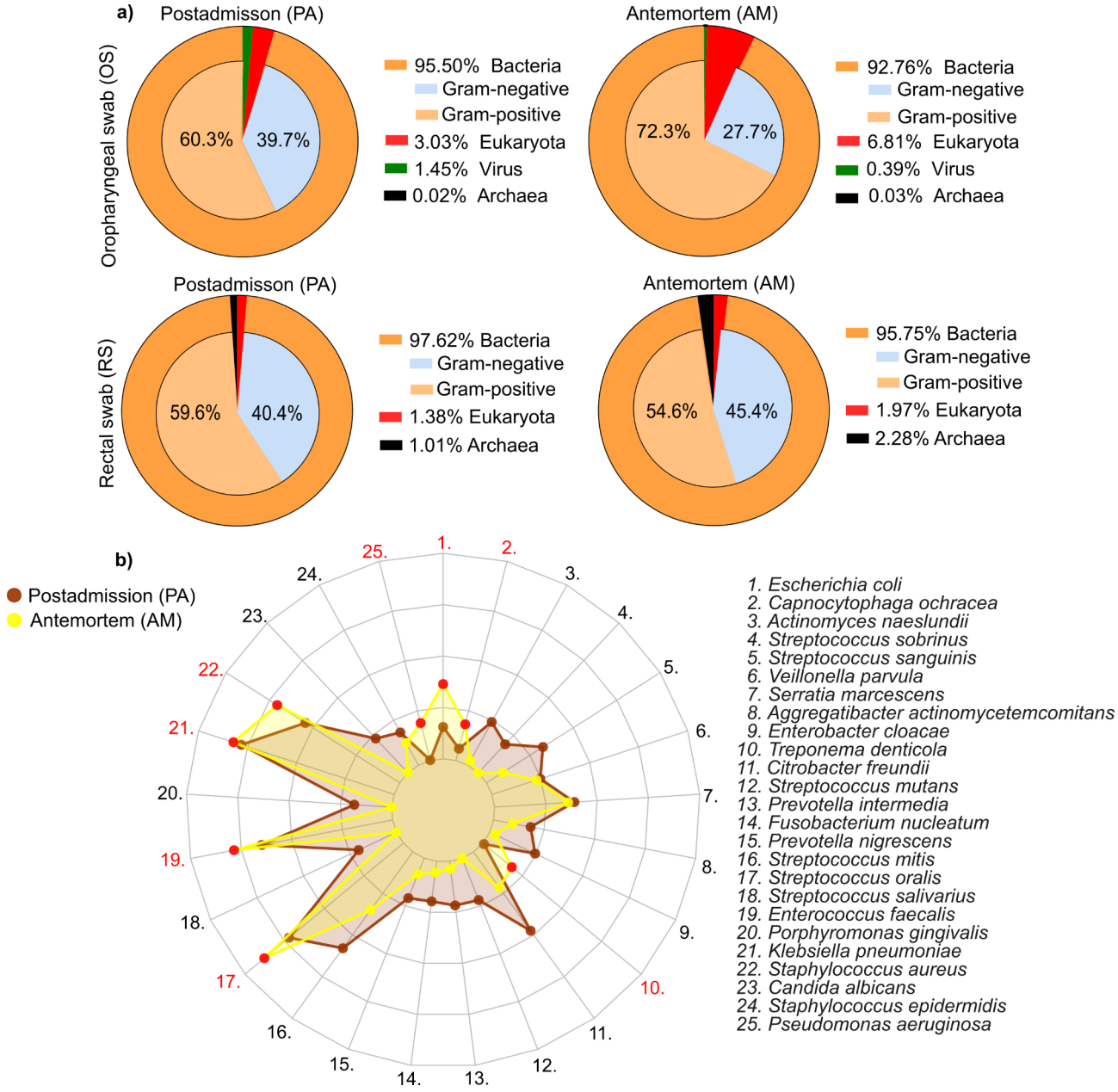

Fig. 2. Comparative analysis of microbiota in oropharyngeal and rectal swabs of ICU patients. Temporal shifts in gram-negative and gram-positive bacteria, eukaryota, viruses, and Archaea in (**a**) the oropharyngeal and rectal swab samples shown in a pie chart. (**b**) The radar chart illustrates changes in the abundance of biofilm-forming bacterial species in antemortem samples relative to postadmission samples. Each axis represents a different biofilm-forming species, and the chart depicts fluctuations in bacterial abundances over time. Biofilm-forming species with an increased abundance in antemortem samples are indicated in red.

compared with that in postadmission samples. However, we did not observe the same trend in rectal swab samples, where the proportions of eukaryotes remained unchanged (PA: 1.38% ± 0.019 vs. AM: 1.97% ± 0.028), with only a mild increase observed. In the RS samples, we observed an increase in the proportion of *Archaea*, which can be referred to as a doubling effect on average (PA: 1.01% ± 0.24 vs. AM 2.28% ± 0.55). However, in the OS samples, the *Archaea* ratios remained virtually unchanged (PA: 0.02% ± 0.002 vs. AM: 0.03% ± 0.002). No viruses were detected in the RS samples, whereas in the OS samples, their proportion nearly quartered, with an average decrease of 1.06% ± 0.012. Changes in the 25 most common biofilm-forming species in oropharyngeal microbiome swab samples were also examined (Fig. 2b). The results revealed that their proportion increased slightly in antemortem states compared with postadmission conditions, but this increase was not significant (0.0045 ± 0.031 vs. $5.67^{*}10^{-5} \pm 2.67^{*}10^{-4}$, P value: 0.0972). This increase can be attributed to the increasing trends in the proportions of eight species, including *Escherichia coli* (2.31x), *Capnocytophaga ochracea* (3.06x), *Treponema denticola* (23.86x), *Streptococcus oralis* (1.2x), *Enterococcus faecalis* (1.21x), *Klebsiella pneumoniae*

(1.05x), *Staphylococcus aureus* (1.3x), and *Pseudomonas aeruginosa*, the latter showing a 90.16-fold increase and the lowest occurrence alongside *Streptococcus oralis* (*S. oralis* PA showing 0.00094 ± 0.00087 and *P. aeruginosa* PA at 0.0008 ± 0.0008). Only *E. coli* exhibited a significant increase from postadmission: 0.062 ± 0.135 to 0.144 ± 0.277 (P value 0.0158).

A remarkable decrease in diversity was observed in the severely dysbiotic antemortem rectal swabs

There was a weak correlation between microbial diversity in postadmission oropharyngeal and rectal swab samples and disease severity, as classified by APACHE II scores (p values: OS: 0.34, RS: 0.35) (Fig. 3a), with correlation coefficients of 0.3 for oropharyngeal swabs and 0.21 for rectal swabs. PCoA analyses were conducted to explore potential taxonomic differences in the microbial compositions of oropharyngeal and rectal swabs from postadmission and antemortem sample fractions (Fig. 3b). Based on the taxonomy data, the PA and AM samples were evenly distributed across the two identified clusters (Clusters 1 and 2), indicating that there was no significant variation in community composition. The changes in the microbiota present in oropharyngeal and rectal swab samples collected postadmission and antemortem were analyzed via Shannon diversity indices, as shown in Fig. 3c. In both cases, there was a decrease in diversity, but it was nonsignificant. The diversity of rectal swab (RS) samples was greater postadmission (3.073 ± 0.546) than that of oropharyngeal swab (OS) samples (2.314 ± 0.665). The diversity of the RS samples decreased to 2.915 ± 0.26 antemortem, whereas the diversity of the OS samples decreased to 1.936 ± 0.215 antemortem. The proportions of anaerobes (Fig. 3d) and potential pathogens (Fig. 3e) were further investigated. Consistent with our previous findings, there were no visibly distinguishable differences in the distributions of anaerobes and potential pathogens between the oropharyngeal and rectal swab communities when postadmission samples were compared with heavily dysbiotic samples from deceased antemortem patients. In general, a gradient-like distribution was observed in the samples on the 2-dimensional plots, although this pattern was less pronounced for potential pathogens.

Estimating strain sharing rates between oral and intestinal microbiota in critically ill patients

The extent of microbiota overlap between oropharyngeal and rectal swab bacteriomes was investigated in critically ill patients to evaluate the impact of the interconnectedness of microbiota colonizing different anatomical sites. To quantify patterns of vertical transmission, a Venn diagram was generated to depict the proportion of shared taxonomic units (Fig. 4). A total of 50.6% of the taxonomic units (7371) were commonly shared, encompassing 453 bacterial classes, 738 bacterial orders, and 2798 bacterial genera (Fig. 4a). The proportion of noncohabiting microbiota was greater in the oropharyngeal swab samples (OS), with 4141 taxonomic units, than in the rectal swab samples, with 3,056 taxonomic units, accounting for 28.4% and 21.0% of all strains, respectively. The cohabiting microbiota between oropharyngeal and rectal swab samples was further analyzed, examining the relative abundance of the 10 most dominant bacteria across three key taxonomic levels: class, order, and genus (Fig. 4b). Notably, the primary classes observed were *Bacteroidia* (40.96%), *Clostridia* (29.85%), and *Bacilli* (11.58%), and *Gammaproteobacteria* (11.96%). Nearly identical proportions were noted for *Bacilli* (OS: 6.06% vs. RS: 5.52%), *Betaproteobacteria* (OS: 1.08% vs. RS: 1.56%), and *Negativicutes* (OS: 1.5% vs. RS: 0.93%). The most prevalent orders included *Bacteroidales* (40.94%) from *Bacteroidia*, *Eubacteriales* (27.08%) and *Lactobacillales* (7.76%) from *Bacilli*, and *Enterobacteriales* (7.26%) from *Gammaproteobacteria*. The *Verrucomicrobiales* order from the *Verrucomicrobiae* class presented similar relative abundances in both the OS and RS samples (0.18% vs. 2.88%). At the genus level, *Bacteroides* (8.46%), *Enterococcus* (3.78%), and *Alistipes* (4.56%) were most abundant in the RS samples, whereas the OS samples presented increased prevalence rates of *Prevotella* (5.23% vs. 3.11%), *Pseudomonas* (3.06% vs. 0.40%), and *Streptococcus* (1.9% vs. 1.25%). Overall, similar trends were observed across the three taxonomic levels, with the changes in the proportions of the 10 most common core community constituents following roughly identical trends.

Identification of differentially abundant microbes (DAMs) in severely dysbiotic antemortem microbiota

Temporal variations were observed in 100% of the core microbiomes of both oropharyngeal and rectal swabs from the time of admission to the antemortem period. Community constituents were identified as showing significant changes in their relative frequencies (Fig. 5). A Venn diagram was generated to compare oropharyngeal- and rectal swab microbiota and to visualize shared and unique taxonomic units (Fig. 5a). Notably, oropharyngeal samples presented a greater total number of taxonomic units than rectal swabs (OS: 11512 vs. RS: 10427). The proportion of shared taxonomic units was similarly high in both sample types, with 71.25% (8203 taxonomic units) in the OS samples and 70.41% (7342 taxonomic units) in the RS samples. For the OS samples, 18.58% of the taxonomic units were found exclusively in the postadmission samples, whereas 10.16% were unique to the antemortem samples. In the RS, 16.49% of the taxonomic units were unique to postadmission samples, with 13.10% unique to antemortem samples. Intriguingly, the number of unique taxonomic units in OS antemortem samples was greater than that in the RS samples. Volcano analyses were utilized to identify differentially abundant microbes (DAMs) that represented significant shifts in their relative frequencies among the shared taxonomic units (Fig. 5b). According to the volcano analysis of oropharyngeal swab (OS) samples, 122 community members (comprising 51 species, 32 genera, 26 families, 9 orders, 3 classes and 1 phylum) significantly increased, whereas 86 community members (including 30 species, 19 genera, 14 families, 12 orders, 5 classes, 4 phyla and 1 kingdom) significantly decreased in antemortem samples compared with postadmission. Based on these findings, at the species level, 8 bacterial and fungal species were significantly more common in antemortem samples than in postadmission samples, whereas the relative occurrence of 15 bacterial and fungal species was significantly lower in antemortem samples than in postadmission samples (Fig. 5a). For the rectal swab (RS) samples, 61 community members (consisting of 28 species, 16 genera, 11

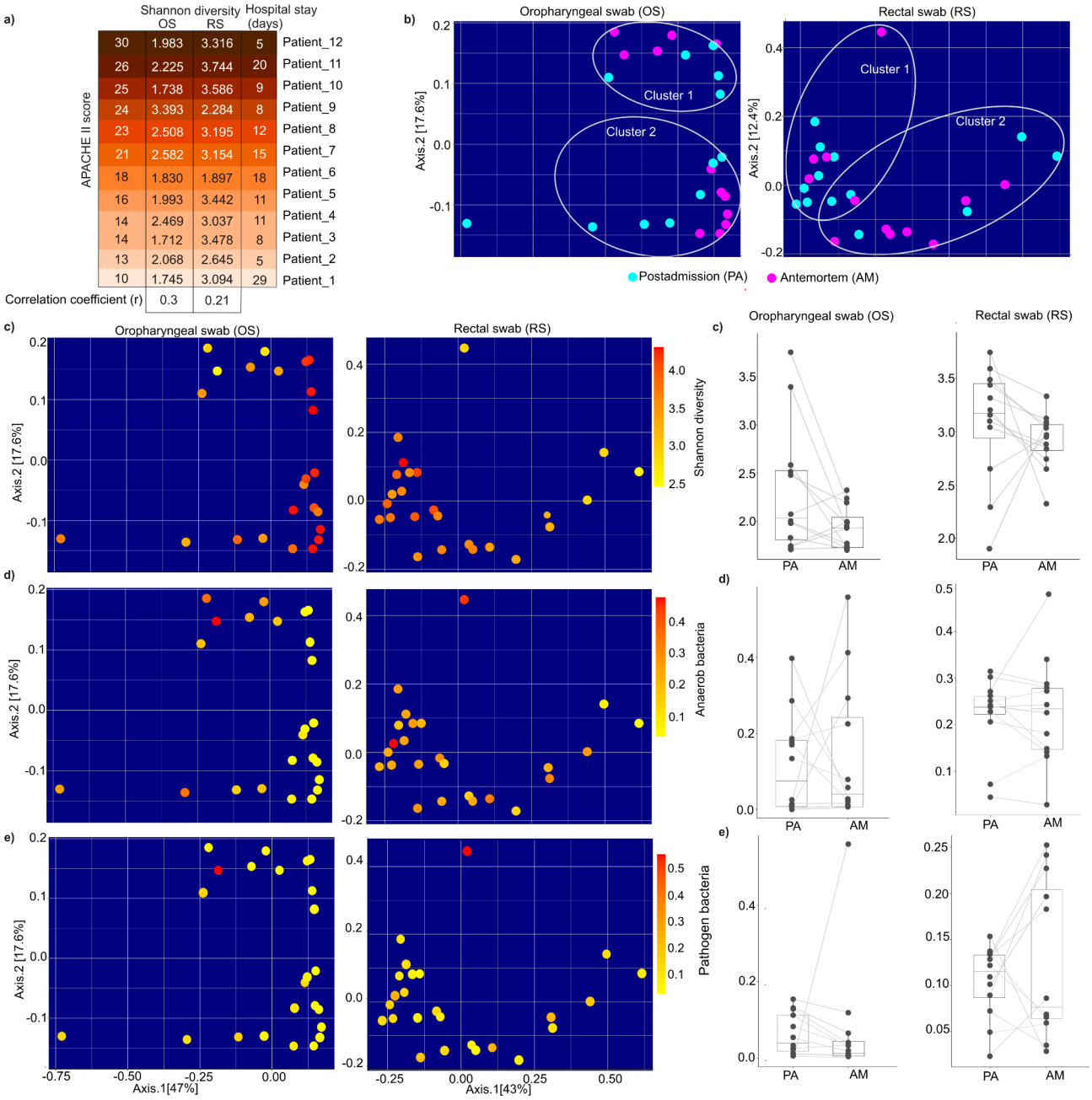

Fig. 3. A remarkable reduction in microbial diversity was observed in the rectum, but not in the oropharynx, in antemortem samples compared with postadmission samples. (**a**) A table was made to demonstrate the patients' APACHE II scores, diversity values, and the number of hospital stay in the postadmission oropharyngeal and rectal swab samples. PCoA plots were created to investigate potential clustering pattern similarities between oropharyngeal swab (OS) and rectal swab (RS) results when comparing (**b**) postadmission (PA) and antemortem (AM) sample populations, (**c**) Shannon diversity, (**d**) anaerobes and (**e**) potential pathogens. Points in PCoA plots were calculated based on quantitative Bray–Curtis statistics and are colored according to a gradient scale of the (**c**) Shannon diversity indices, d) relative abundance of anaerobic bacteria, and (**e**) relative abundance of pathogenic bacteria. In every case, box plots were used to examine the significant differences between the sample fractions (PA vs. AM). Statistical significance was determined by the Wilcoxon matched-pairs signed rank test (n.s. nonsignificant).

families, 3 orders and 3 classes) presented significant increases, whereas 79 community members (comprising 37 species, 20 genera, 10 families, 6 orders, 4 classes and 2 phyla) presented significant decreases in antemortem samples compared with postadmission samples (Fig. 5c). Accordingly, at the species level, 9 bacterial species were found to significantly increase, whereas 25 bacterial species significantly decreased in the antemortem samples relative to the postadmission samples.

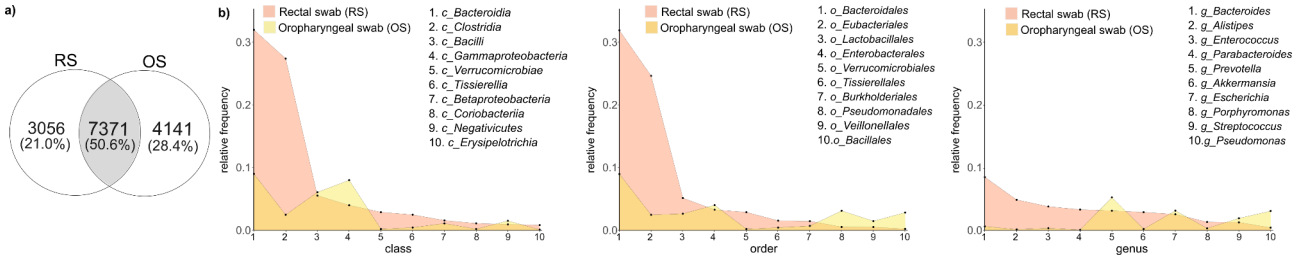

Fig. 4. Analysis of transmission patterns of bacterial taxonomic units in oropharyngeal and rectal swabs. (**a**) A Venn diagram was generated to measure the taxonomic units present in both oropharyngeal and rectal swab samples to identify the common microbial populations across the anatomical sites. (**b**) Area plots illustrating the proportions of the 10 most frequent coexisting bacteria in oropharyngeal and rectal swab samples, highlighting the overlap in these distinct anatomical locations across classes, orders and genera.

Highly interconnected microbial species in severely dysbiotic oropharyngeal and rectal swabs

Two distinct approaches were used to identify interconnected microbial biomarker species in both the oropharynx and rectum whose relative abundances could potentially characterize severely dysbiotic microbial states observed in deceased patients' samples prior to their death (Fig. 6). Based on their strong correlations ($r > 0.7$), either member of the interconnected biomarker species could serve as a potential predictor of severe dysbiosis by mutually indicating the presence of the other. Thus, a more easily detectable oropharyngeal species could signal microbial shifts in the gut, which may be more challenging to assess directly, especially in critically ill patients. This interconnection offers clinicians a practical approach to monitor gut dysbiosis via accessible oral samples, providing an early detection method. According to the first approach, interconnected differentially abundant microbes (DAMs) were identified as consistently detectable in both postadmission and antemortem samples of moderately and severely dysbiotic microbiomes, respectively. However, by exhibiting significantly different abundance levels between these states, they can have a potential role in indicating the progression of dysbiosis (Fig. 6a). In the second approach, unique interconnected microbial biomarker species, exclusively found in antemortem samples, were identified, characterizing severely dysbiotic states (Fig. 6b). A total of seven DAMs whose relative occurrence was strongly correlated with nine species in rectal swab microbiomes were identified (Fig. 6a). The strongest correlation was detected between OS *Actinomyces dentalis* and RS *Alloscardovia omnicolens* (r = 0.922). Two oropharyngeal species were strongly correlated with two rectal swab species each: *Leptotrichia wadei* (with *Roseburia inulinivorans* r: 0.846, *Anaerococcus rubeinfantis* r: 0.717) and *Rothia dentocariosa* (with *Neofamilia massiliensis* r: 0.734, *Anaerococcus rubeinfantis* r: 0.823). Furthermore, the correlations included OS *Citrobacter braakii* with RS *Treponema phagedenis* (r: 0.735), OS *Enterobacter mori* with RS *Corynebacterium aurimucosum* (r: 0.874), and OS *Veillonella rogosae* with RS *Coprobacter fastidiosus* (r: 0.749). Among the species that emerged uniquely in severely dysbiotic antemortem samples (Fig. 6b), *Hoylesella nanceiensis* and *Gemella haemolysans* were the two species with the greatest number of strong correlations with rectal swab species. *H. nanceiensis* was strongly correlated with the SCFA producers *Clostridium butyricum* and *Corynebacterium* species. *Legionella pneumophila* also emerged in the patient's oropharyngeal samples, which may be attributed to the severely dysbiotic condition of the oropharyngeal microbiota.

Modularity and density dynamics in the microbial networks of critically ill patients' stressed microbiomes

Network analyses were employed to explore the alterations in microbial community interactions (Fig. 7). In oropharyngeal swabs, a greater degree of modularity was noted in postadmission samples (OS PA modularity: 0.35) than in antemortem samples (OS AM modularity: 0.13), indicating a 2.69-fold reduction in modularity from PAs to AMs (Fig. 7a). However, in the case of the rectal swabs, we observed an increase in modularity from 0.19 in the PA samples to 0.53 in the AM samples, indicating a 2.78-fold increase. This variation is mirrored in the graph structures for the OS PA and RS AM samples, which are organized into distinct modules characterized by denser intramodule connections and sparser intermodule connections. Density trends developed in contrast to the modularity values, as if to counterbalance the low modularity, in both oropharyngeal and rectal swab samples. We observed that low modularity typically correlated with higher density values. Accordingly, for the OS samples, we measured greater density in the severely dysbiotic antemortem case than in the postadmission case (density OS PA: 0.17 vs. OS AM: 0.37, a 2.17-fold difference). The trends for rectal swabs were opposite those for oropharyngeal swabs; however, to counterbalance lower modularity, we measured higher density in the less dysbiotic postadmission samples than in the more modular but more dysbiotic antemortem samples (density RS PA: 0.25 vs. RS AM: 0.07, a 3.57-fold difference). Interestingly, when the proportion of actual connections in the networks was measured, the highest density (density: 0.37) was present in oropharyngeal antemortem samples. Considering the pivotal role that keystone taxa play in shaping the resilience of microbial communities, they could act as microbial biosensors for characterizing various dysbiotic states. Notably, in our study, we identified specific keystone taxa within severely dysbiotic oropharyngeal antemortem samples that were not recognized as nodes in either the rectal swabs or the less dysbiotic oropharyngeal swab samples (Fig. 7b). Among these were two phyla: *Pseudomonadota* (degree of node value: 0.68) and *Chlamydiota* (degree of node value: 0.64);

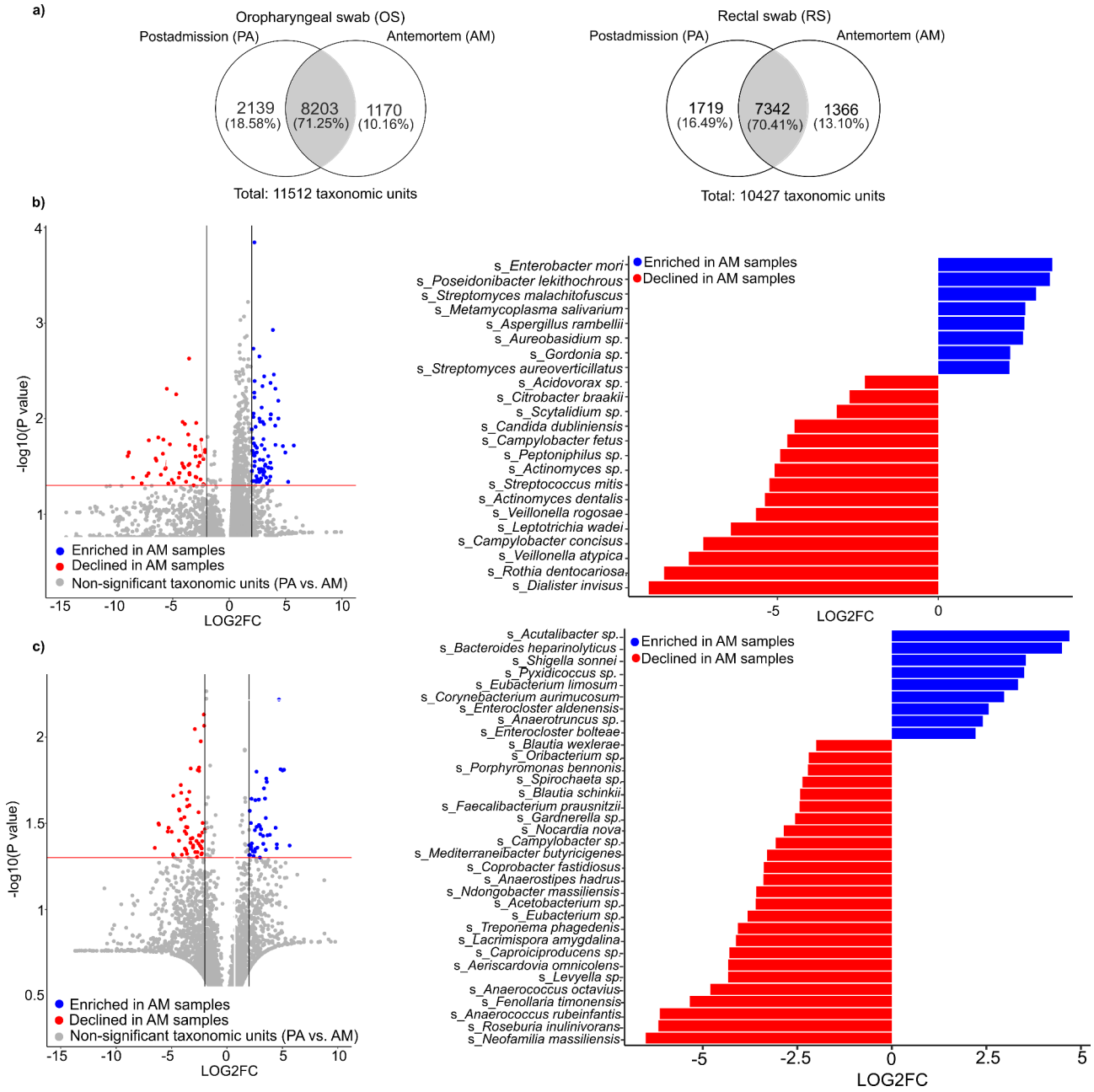

Fig. 5. Differentially abundant microbes (DAMs) in 100% of the cores from oropharyngeal and rectal swabs. (**a**) Comparative analysis of shared and unique microbial populations between postadmission and antemortem swab samples from ICU patients was conducted via Venn diagrams for both oropharyngeal and rectal swabs. (**b**) and (c) Volcano analyses were performed to identify significant microbial shifts in ICU patients by comparing postadmission samples with antemortem samples among oropharyngeal and rectal swab samples, respectively. The volcano plot represents the DAMs showing statistically significant overexpression and underexpression (according to the log2-transformed fold change in relation to the -log10-transformed P value). The dashed line on the y-axis indicates the -log10P value = 1.301 threshold, with statistically significant ($P < 0.05$) higher (blue) and lower abundances (red). In each analysis, bar plots illustrate the differentially abundant microbes (DAMs) that were significantly enriched (blue) or depleted (red) in antemortem samples.

two orders: *Enterobacterales* (degree of node value: 0.59) and *Desulfobulbales* (degree of node value: 0.64); three genera: *Pseudomonas* (degree of node value: 0.67), *Klebsiella* (degree of node value: 0.60), and *Bacillus* (degree of node value: 0.62); one family: *Chlamydiaceae* (degree of node value: 0.58); and two classes: *Gammaproteobacteria* (degree of node value: 0.69) and *Chlamydiia* (degree of node value: 0.64), all of which represent similar but the highest degree of node values in our sample population. This occurred despite their identification as keystone taxa within a network characterized by the lowest modularity in the population. Except for one node (*Alistipes*), we observed a similar pattern in the rectal swab samples, where we identified 9 nodes that exclusively appeared

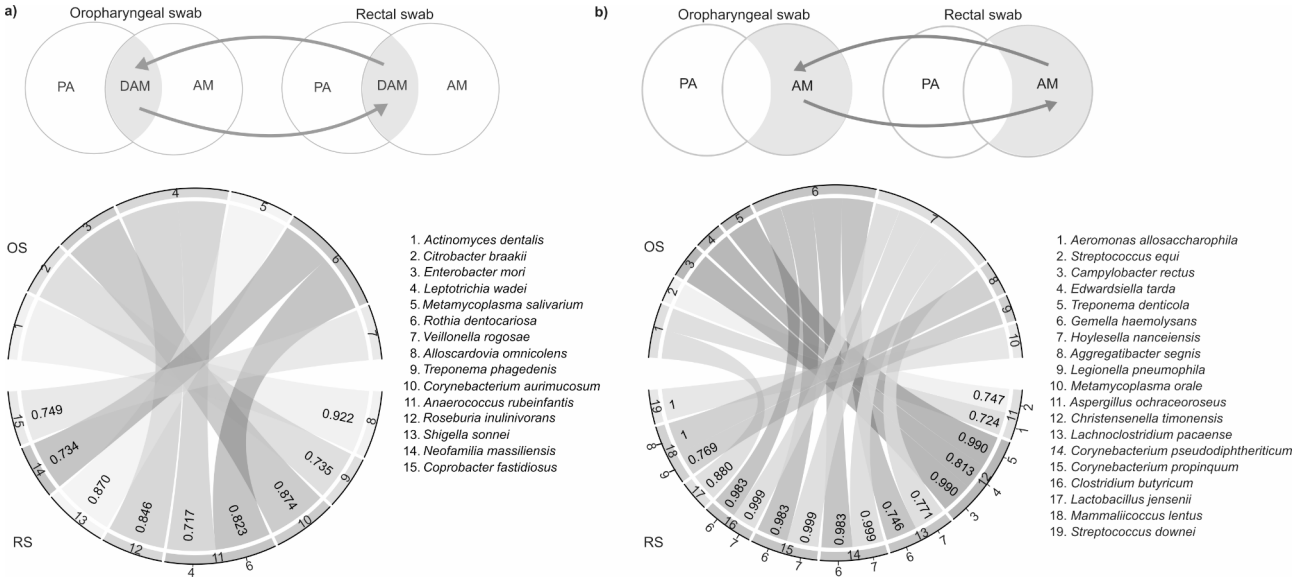

Fig. 6. (**a**) Upper panel: Venn diagram showcasing intersected differentially abundant microbes (DAMs) consistently detectable in both post-admission and antemortem samples of moderately and severely dysbiotic microbiomes. Arrows point to DAMs present in both oropharyngeal (OS) and rectal swab (RS) samples, marking key overlaps across sampling sites. Bottom panel: Chord diagram illustrating species with strong positive correlations (Pearson correlation coefficient > 0.7) between oropharyngeal swab (7 species) and rectal swab (9 species) samples, highlighting interconnected microbes across these anatomical regions. This interconnectivity suggests potential microbial biosensors for severe dysbiosis across sample types. (**b**) Upper panel: Venn diagram highlighting unique interconnected microbial biomarkers exclusively identified in antemortem samples, with arrows denoting species strongly associated with severely dysbiotic states. Their distinct presence underscores their diagnostic potential for characterizing advanced dysbiosis stages. Bottom panel: Chord diagram demonstrating species with strong positive correlations (Pearson correlation coefficient > 0.7) between oropharyngeal swab (10 species) and rectal swab (9 species) samples, reflecting high interconnectivity across anatomical regions. These interconnected species suggest microbial biosensors that could indicate severe dysbiosis in both sample types.

as keystone taxa within that network architecture. These included 1 order: *Campylobacterales* (degree of node value: 0.46); 4 families: *Clostridiaceae* (degree of node value: 0.48), *Coriobacteriaceae* (degree of node value: 0.40), *Lachnospiraceae* (degree of node value: 0.50), *Oscillospiraceae* (degree of node value: 0.48); and 4 genera: *Ruminococcus* (degree of node value: 0.44), *Corynebacterium* (degree of node value: 0.45), *Campylobacter* (degree of node value: 0.46), and *Blautia* (degree of node value: 0.46). Finally, the genus *Alistipes* was the only one identified as a keystone taxon based on oropharyngeal postadmission samples, albeit with a smaller degree of nodes (degree of node in OS PA: 0.26 vs. RS PA: 0.48). According to the network architecture of the rectal swab samples, which was characterized by the highest modularity, the keystone taxa on average presented the smallest degree of node values. Among these, only two were unique, meaning that only these keystone taxa were identified across these network structures (class *Methanobacteria* and the genus *Parabacteroides*, both showing the same degree of node values at 0.18).

Discussion

In critically ill patients, underlying health conditions, the frequent need for invasive procedures, and multiple drug therapies compromise physical defenses. This can worsen dysbiosis, allowing pathogens to invade and cause severe, potentially life-threatening infections[24].

In our longitudinal study, we analyzed microbiome samples from 12 critically ill patients who died in the intensive care unit. By sampling every three days, we traced dysbiosis progression up to the day of or three days before death during the ICU stay, enabling us to compare the initial postadmission samples directly with those collected antemortem.

Samples were collected from two specific anatomical sites: the oropharynx and rectum. The rationale for including both rectal and oral samples was based on increasing evidence that microbial communities across various anatomical sites are interconnected[25]. Specifically, the oropharyngeal and rectal microbiomes display correlated shifts, offering a more holistic understanding of the dysbiotic processes occurring throughout the body[11]. Furthermore, given that oropharyngeal samples are more easily accessible in most cases, they could serve as early indicators of deteriorating microbial changes in the gastrointestinal tract—an area that is more difficult to assess, particularly in critically ill patients. Therefore, a deeper understanding of these interconnections between the oropharyngeal and rectal microbiota may also be valuable for future interventional research by offering insights into the relationship between dysbiosis progression and the development of infections in ICU

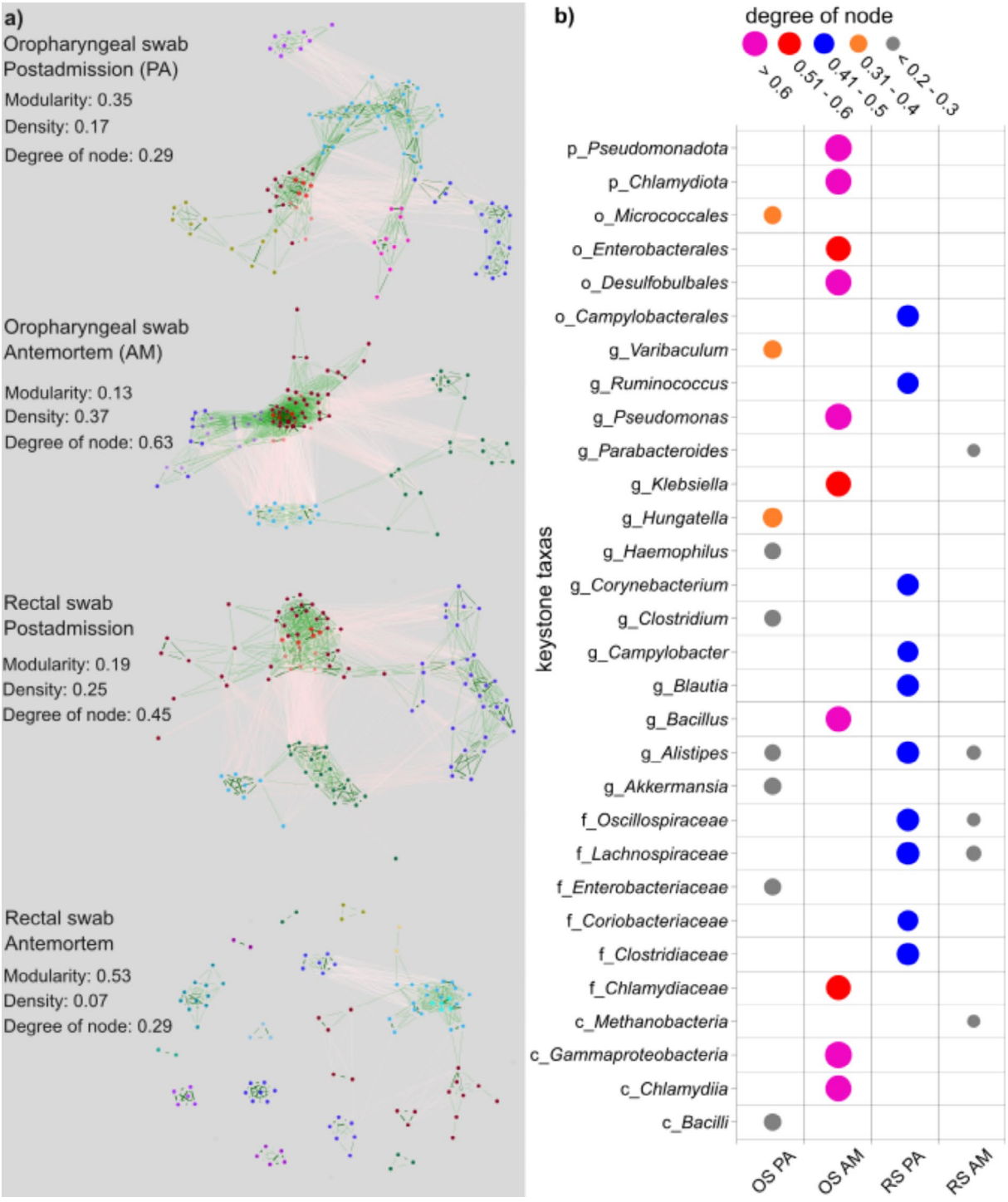

Fig. 7. Figure demonstrating the differences in microbial community structures and interactions between sample types and times (postadmission vs. antemortem). (**a**) Four network graphs are represented to illustrate the complex structures of microbial communities within different sample types and collection times: oropharyngeal swab postadmission (OS PA), oropharyngeal swab antemortem (OS AM), rectal swab postadmission (RS PA), and rectal swab antemortem (RS AM). Each graph details the network's modularity, density, and degree of nodes. (**b**) Degree of node values for keystone microbial taxa. The legend on the right indicates the presence and abundance of taxonomic units with various colors, where larger nodes may indicate more dominant or abundant species. The circle sizes in the graph correlate with the degree of a node, with the smallest circles representing values under 0.3, increasing incrementally through ranges of 0.31–0.4, 0.41–0.5, 0.51–0.6, and exceeding 0.6. The diversity in node degree reflects the varying influence of different taxa within the microbial communities. The network correlations and degrees of nodes were determined via Pearson correlations.

patients. By analyzing microbial swabs of both anatomical sites, we aimed to provide a more comprehensive perspective on these disruptions.

Swabs are accepted as a method of sample collection and have been demonstrated to be closely comparable with the gut bacterial composition and alpha diversity[26–29]. For our investigations, oropharyngeal and rectal swab samples were utilized to address these challenges. Microbiome profiles collected immediately postadmission were considered as dysbiotic, whereas antemortem samples taken shortly before death presented severe dysbiosis. Based on our data no significant correlation was observed between the duration of hospital stay and the onset of death, indicating that the duration of ICU hospitalization alone does not serve as a reliable prognostic marker for increased mortality risk in critically ill patients.

The distribution of taxonomic units among bacteria, Archaea, eukaryotes, and viruses to identify the characteristics of severely dysbiotic microbiomes was also analyzed. To draw comprehensive conclusions, antemortem samples were systematically compared with postadmission samples using oropharyngeal and rectal swabs from our patient cohorts. Our findings revealed a decrease in the proportion of bacteria in both oral and rectal swab samples from admission to patient death. During the observation period, the proportion of gram-positive bacteria found in oropharyngeal swab samples from deceased patients significantly increased.

The oral cavity is home to a diverse array of gram-positive bacteria, including species from the *Streptococcus*, *Staphylococcus*, and *Enterococcus* genera. Consequently, the observed increase in certain microbes known to cause primary endogenous infections, such as biofilm-producing *Streptococcus oralis*, *S. pneumoniae*, methicillin-resistant *Staphylococcus aureus* (MRSA), coagulase-negative *Staphylococci*, and *Enterococcus faecalis*, may contribute to a greater proportion of gram-positive bacteria in the oropharynx[30,31]. In RS samples the *Archaea* ratio doubled, whereas in OS samples, it remained unchanged. With respect to viruses, no viruses were found in the RS samples, whereas a decrease was observed in the OS samples.

The comparison between antemortem and postadmission swab samples revealed reduced diversity in both the oropharyngeal and rectal swab microbiota. Our findings partly align with previous studies on the diversity of the gut and oropharyngeal microbiota in ICU patients, which revealed a wide range of Shannon diversity indices from 1.29 to 4.5[4,21,32–40]. Unlike these studies, our lowest recorded Shannon diversity indices were higher for both oropharyngeal and rectal swabs. The relatively high resilience of the rectal swab microbiota highlights its crucial role in adaptability.

We found that critically ill patients experienced significant changes in eukaryotic populations in their oropharyngeal microbiota, with the proportion of eukaryotes in OS more than doubling. In contrast, rectal swabs showed minimal changes. Based on our observations, clinical interventions facilitating the proliferation of eukaryotic organisms are more pronounced in the oropharyngeal area. This finding may also imply that increased eukaryotic biomass in oropharyngeal samples from ICU patients may be associated with worsening health outcomes.

Interestingly, despite 67% of the population experiencing septic shock, we found no significant alterations in potential infection-causing microorganisms.

Among the key beneficial bacteria, various species of *Bacteroides* play crucial roles in breaking down polysaccharides and oligosaccharides, thus providing nutrients and vitamins to the host[41]. While they play a role in maintaining microbial balance, certain species within the genus *Bacteroides* can become pathogenic in the oral cavity, highlighting their intricate role in health and disease[42]. The *Bacteroides* genus was significantly more abundant in the intestine, as evidenced by its 14-fold greater presence in rectal swab samples than in oropharyngeal swab samples. Additionally, the genus *Enterococcus* was found to be significantly more prevalent in rectal swab samples, being 11.45 times more abundant than in oropharyngeal swab samples. *Enterococcus* species, including *Enterococcus faecalis* and *Enterococcus faecium*, are part of the normal eubiotic microbiota. However, they can turn into opportunistic pathogens, particularly in hospital environments[43]. This characteristic underscores the importance of monitoring their presence, as they may contribute to healthcare-acquired infections, especially in individuals with compromised health[44]. The *Prevotella* genus was more abundant in oropharyngeal swab samples, where it constituted 5.23%, than in rectal swabs, which constituted 3.11%. This represents a 1.68-fold increase. Saliva, particularly, is highly diverse within the *Prevotella* genus. As a key anaerobic genus within the oral microbiome, *Prevotella* species are part of the microbial communities in both the gastrointestinal and respiratory tracts outside the oral cavity[45,46]. However, at the species level, most existing research has focused on *P. intermedia* and *P. nigrescens* because their importance is associated with a dysbiotic oral microbiota[46]. In severely dysbiotic communities extending beyond the oral cavity, through hematogenous spread, *Prevotella* can impact a wide range of body sites, causing infections in the gastrointestinal, respiratory, and urogenital tracts; skin; central nervous system; and bloodstream[47].

Strain-sharing rates between the 100% core microbiota at two distinct anatomical sites—the oropharynx and the intestine—were also assessed. Significant microbiota overlaps were found, with a core set of abundant microbial strains suggesting 'mutual vertical transmission'. Better understanding strain-sharing rates is crucial for infection control, especially in intensive care units where patients are more susceptible to infections due to compromised barriers and immune defenses.

Strongly interconnected OS-RS species pairs were also identified, whose presence and abundance in our cohort were characteristic of more severely dysbiotic microbiomes, as determined by comparison with postadmission samples. Through our analysis of differentially abundant microbes (DAMs) being present in both postadmission and antemortem samples, microbes were identified in the oropharyngeal and rectal swabs showing significantly different abundances between the two sampling stages. These findings help highlight the shifts in microbial communities as the patient's condition worsens, progressing from moderately dysbiotic microbiomes to severely dysbiotic states. Additionally, in the postadmission samples, common microbes were identified whose presence was exclusively characteristic of the more severely dysbiotic microbial swabs, showing a strong correlation in both OS and RS samples. Seven oropharyngeal microbes (*Actinomyces dentalis*,

Citrobacter braakii, *Enterobacter mori*, *Leptotrichia wadei*, *Metamycoplasma salivarium*, *Rothia dentocariosa*, and *Veillonella rogosae*) significantly increased in abundance in patients experiencing severe dysbiosis, and these microbes demonstrated strong correlations (correlation coefficient > 0.7) with nine analogous microbes (*Alloscardovia omnicolens*, *Treponema phagedenis*, *Corynebacterium aurimucosum*, *Anaerococcus rubeinfantis*, *Roseburia inulinivorans*, *Shigella sonnei*, *Neofamilia massiliensis*, *and Coprobacter fastidiosus*) found in rectal swabs. *Leptotrichia* species in the oropharynx are facultative anaerobes that are primarily found in the oral cavity and act as opportunistic pathogens in conditions such as mucositis and oral lesions[48]. *L. wadei* can cause septicemia in individuals with predisposing factors and has been isolated from both immunocompromised and immunocompetent hosts[48]. *Rothia* species are commensals in the human mouth that contribute to oral health[49]. *Citrobacter braakii* is known as an anaerobic, gram-negative bacterium that is associated with acute mucosal inflammation, especially in the stomach[50], and is correlated with *Treponema phagedenis* in the gut.

Certain species, such as *Hoylesella nanceiensis* and *Gemella haemolysans*, were significantly correlated with SCFA-producing counterparts, such as *Clostridium butyricum* and *Corynebacterium* species, in the rectal swab microbiota. These findings suggest that these genes might play a role in either compensatory mechanisms or opportunistic expansions within the dysbiotic environment. Additionally, the presence of *Legionella pneumophila* in oropharyngeal samples suggests that dysbiosis may create an environment that might facilitate the growth and proliferation of certain pathogens.

In this study, the strong correlations found between the oropharyngeal and rectal microbiomes further underscore the valuable interconnectedness of human microbial ecosystems, which is particularly relevant in critically ill patients. In these patients, dysbiosis in one anatomical site may serve as an indicator of broader microbial imbalances across multiple sites.

System-level changes were monitored to decipher the structures of microbial communities, particularly focusing on those detected within antemortem sample populations in comparison to postadmission ones across both oropharyngeal (OS) and rectal swab (RS) communities. These analyses aimed to capture the changes in community resilience as patients' conditions deteriorated. Modularity was assessed, denoting the network's segmentation into subcommunities, thus revealing the existence of functional clusters, i.e., groups of microbes that potentially collaborate within specific metabolic pathways[51]. High modularity within a network is an indicator of resilience, as it isolates disturbances to specific modules, thereby preventing widespread system failure[52]. This compartmentalization confers functional redundancy, ensuring that essential biological processes endure despite the loss of individual species and, thus bolstering the intestinal microbiota's resilience to the demanding conditions of the ICU[53]. Based on our data the microbial communities in the oropharynx of deceased patients exhibited a low level of modularity, indicating that they are more prone to systemic disturbances.

Our data indicate an inverse correlation between modularity and density in dysbiotic communities, suggesting a potential compensatory mechanism in which increased network density may compensate for decreased modularity, thus maintaining the functionality and stability of microbial ecosystems.

In conclusion, our findings indicate that strategies aimed at regenerating oropharyngeal microbiomes could have a considerable impact on the health and stability of intestinal microbiomes, thereby potentially influencing the recovery outcomes of critically ill patients.

It is important to emphasize that, although we successfully identified biomarkers that exhibited characteristic patterns in our severely dysbiotic sample populations, they should not necessarily be considered directly causative of the observed dysbiosis. However, the stable and distinct presence of these microorganisms, along with their consistent detection in both the oropharynx and rectum, provides a strong foundation for further research. This could involve investigating biomarkers that enable predictions of microbial changes in one anatomical region based on the presence or variation of biomarkers in another, potentially correlating these changes with the progression of dysbiosis.

Materials and methods

Study design and subjects

A retrospective longitudinal cohort study was carried out, in which oropharyngeal and rectal swab microbiome samples were collected from 69 adult patients admitted to the Central Anesthesia and Intensive Care Unit of Markusovszky University Teaching Hospital, Szombathely, between 15 February 2023 and 22 June 2023. Inclusion criteria required adult, deceased patients admitted to the ICU ward, with an anticipated stay of at least 48 h. 12 adult patients (8 males, 4 females) met the criteria with a mean age of 68.67 ± 10.85 and had a median hospital stay of 11 days (range, 5–29 days). Throughout their stay in the ICU, patients' samples were systematically collected at three-day intervals to obtain antemortem samples from deceased patients one or two days prior to death. The samples were categorized into two groups by pairing each patient's samples: those collected upon admission to the ward (postadmission) and the last samples taken before death (antemortem); the remaining samples were not considered. A total of 48 swab samples were collected: 12 postadmission oropharyngeal swab samples, 12 antemortem oropharyngeal swab samples, 12 postadmission rectal swab samples, and 12 antemortem rectal swab samples. The sepsis criterion for discerning the study groups was adopted according to the Third International Consensus Definitions for Sepsis and Septic Shock. Nine patients (75%) were diagnosed with sepsis, and among them, sepsis progressed to septic shock in 8 patients, resulting in mortality.

Patients or their relatives were personally informed of the study in the presence of the responsible clinician and signed informed consent forms. The study was approved by the institutional review board of Markusovszky University Teaching Hospital Regional Scientific and Research Ethics Committee with a waiver of informed consent (ethical permission number: 4/2023). All methods were performed following the relevant guidelines and regulations.

Patient sampling and data recording

Rectal and oral swab samples were collected by nurses via brand-sealed sterile, polystyrene, and RNase- and DNase-free swabs (Specimen Collection Swab, Guangzhan MeCan Medical Limited). Fecal samples were collected by dipping the tips into defecated stool as close to the defecation time as possible. Oral swabs were collected by rubbing the swab tips on the surface of the patient's tongue; nurses were instructed to avoid the lips and teeth. These swabs were certified to be DNA free and provided with a 2-ml DNA-free collection tube (Screw cap microtube, Sarstedt, Cat. 72.694.700) containing DNA/RNA transport and storage media (DNA/RNA Shield, Zymo Research, Cat. R1100-250). The swab samples were stored at 4 °C in the hospital and then transported to the laboratory of the University of Debrecen, Faculty of Agricultural and Food Sciences and Environmental Management, Center for Complex Systems and Microbiome Innovations for DNA extraction. The samples were stored at −20 °C until DNA extraction. Demographic, biochemical, and clinical variables of interest, such as age, sex, BMI, glucose, CRP level, ICU venue, sepsis status and SOFA and APACHE-II scores, were collected as patient-associated metadata. Patients' Acute Physiology and Chronic Health Evaluation (APACHE) II scores were assessed, and the average score was 19.5 ± 6.22, ranging from 10 to 30. The APACHE II score is a widely used outcome prediction model in the intensive care setting. During the critical window of the first 24 h postadmission, health care staff carefully assess different physiological parameters of patients. By converting the worst value observed for each parameter into a numerical score ranging from 0 to 71, professionals can indicate how severe the condition is. Higher scores not only indicate more severe disease but also predict a greater chance of death during hospitalization[54,55]. Additional variables associated with the follow-up, such as the type of nutritional support, formula of nutritional support, antibiotic administration, and outcome variables (ICU stay [days], complications in the ICU, discharge condition), were also recorded.

Nucleic acid extraction

DNA extraction from the swab samples was performed via the DNeasy® PowerSoil® Pro Kit (Qiagen, Germany, Cat. 47016) following the manufacturer's instructions. Minor modifications were made to optimize the DNA extraction. In brief, 300 µl of the supernatant was transferred to PowerBead Pro Tubes and incubated at 65 °C for 10 min. With the use of a MagNA Lyser instrument (Roche Applied Sciences, Germany), the samples were lysed two times at 3,000 × g for 30 s. Finally, 70 µl of Solution C6 was added, and the mixture was incubated at room temperature for 5 min before centrifugation. DNA concentrations were determined fluorometrically via a Qubit® Fluorometric Quantitation HS dsDNA Assay (Invitrogen by Thermo Fisher Scientific, Cat. 2600187) kit with a Qubit® 4.0 fluorometer (Thermo Fisher Scientific, USA).

Sequencing and metagenomic data processing

Shotgun sequencing was conducted on an Illumina NovaSeq 6000 instrument (Illumina, USA) with a 150-bp paired-end sequencing run at Novogene Bioinformatics Technology (Beijing, China). The sequencing yielded a minimum of 20 million reads per sample. To ensure the availability of 20 million reads per sample, we reisolated each sample until the required purity (OD260/280 = 1.8–2.0) and concentration ≥ 10 ng/µL for each metagenomic isolate were obtained. Microbial analysis was completed via the SqueezeMeta pipeline (v1.6.3), which uses the coassembly option with no binning[56,57]. The raw reads were quality-filtered with Trimmomatic software (v.0.39) with the following settings: LEADING:8 TRAILING:8 SLIDINGWINDOW:10:15 MINLEN:30. Briefly, paired-end reads were assembled via Megahit. For taxonomic assignment DIAMOND v.2.19 runs were performed against GenBank nr database using a fast LCA algorithm[58–61]. We used the KIFÜ Hungarian High Performance Computing Competence Center (HPC CC) Komondor HPC with 48 CPU cores and 90 GB of RAM per sample.

Statistical analysis and data visualization

To evaluate the species richness and evenness of the samples, the Shannon index was calculated based on the species profile via the phyloseq v.1.44 package in the R program (v.4.4.1)[62,63]. To examine the differences in microbial community structures between groups, PCoA was conducted using the vegan v.2.6-4 package in R[64]. For the volcano analysis, the Wilcoxon rank-sum test was applied, and log2-fold changes were calculated to determine the relative abundances of taxa in antemortem versus postadmission samples. Chord and network diagrams were constructed via Pearson correlation analysis. For statistical test Wilcoxon rank-sum test was used, all statistical tests were two-tailed, and a $P < 0.05$ value was considered statistically significant. The graphs were generated with the R package 'ggplot2' (version 3.5.0) or GraphPad v.8.0.1[65,66]. For microbial network analysis, the NetCoMi R package (v.1.1.0) was used[67,68]. Chord diagrams were visualized with the circlize R package (v.0.4.16)[69,70].

List of potential pathogens and anaerobes

All the potential pathogens and anaerobes used for the analysis were listed in Supplementary File 1, with references for all taxa[42,71–128].

Data availability

All sequence data used in the analyses were deposited in the Sequence Read Archive (SRA) (http://www.ncbi.nlm.nih.gov/sra) under PRJNA1102991.

Received: 12 April 2024; Accepted: 28 October 2024
Published online: 08 November 2024

References

1. Hou, K. et al. Microbiota in health and diseases. *Signal. Transduct. Target. Ther.* **7**, 135 (2022).
2. Willis, J. R. & Gabaldón, T. The human oral microbiome in health and disease: From sequences to ecosystems. *Microorganisms* **8**, 308 (2020).
3. Szychowiak, P., Villageois-Tran, K., Patrier, J., Timsit, J. F. & Ruppé, É. The role of the microbiota in the management of intensive care patients. *Ann. Intensive Care* **12**, 3 (2022).
4. Liu, W. et al. Classification of the gut microbiota of patients in intensive care units during development of sepsis and septic shock. *Genom. Proteom. Bioinform.* **18**, 696–707 (2020).
5. Dickson, R. P. The microbiome and critical illness. *Lancet Respir. Med.* **4** (1), 59–72 (2016).
6. Zulfiqar, M., Singh, V., Steinbeck, C. & Sorokina, M. Review on computer-assisted biosynthetic capacities elucidation to assess metabolic interactions and communication within microbial communities. *Crit. Rev. Microbiol.* 1–40 (2024).
7. Guo, L., He, X. & Shi, W. Intercellular communications in multispecies oral microbial communities. *Front. Microbiol.* **5**, 328 (2014).
8. Little, W., Black, C. & Smith, A. C. Clinical implications of polymicrobial synergism effects on antimicrobial susceptibility. *Pathogens* **10**, 144 (2021).
9. Ponomarova, O. & Patil, K. R. Metabolic interactions in microbial communities: Untangling the Gordian knot. *Curr. Opin. Microbiol.* **27**, 37–44 (2015).
10. Wolff, N. S., Hugenholtz, F. & Wiersinga, W. J. The emerging role of the microbiota in the ICU. *Crit. Care* **22**, 78 (2018).
11. Khor, B. et al. Interconnections between the oral and gut microbiomes: Reversal of microbial dysbiosis and the balance between systemic health and disease. *Microorganisms* **9**, 496 (2021).
12. Mousa, W. K., Chehadeh, F. & Husband, S. Microbial dysbiosis in the gut drives systemic autoimmune diseases. *Front. Immunol.* **13**, 906258 (2022).
13. Kunath, B. J. et al. The oral–gut microbiome axis in health and disease. *Nat. Rev. Microbiol.* (2024).
14. Salameh, T. J. et al. Gut microbiome dynamics and associations with mortality in critically ill patients. *Gut Pathog.* **15**, 66 (2023).
15. Pérez-Cobas, A. E., Baquero, F., de Pablo, R., Soriano, M. C. & Coque, T. M. Altered ecology of the respiratory tract microbiome and nosocomial pneumonia. *Front. Microbiol.* **12**, 709421 (2022).
16. Clasener, H. A. L., Vollaard, E. J. & van Saene, H. K. F. Long-term prophylaxis of infection by selective decontamination in leukopenia and in mechanical ventilation. *Rev. Infect. Dis.* **9**, 295–328 (1987).
17. van der Waaij, D. History of recognition and measurement of colonization resistance of the digestive tract as an introduction to selective gastrointestinal decontamination. *Epidemiol. Infect.* **109**, 315–326 (1992).
18. Freedberg, D. E. et al. Pathogen colonization of the gastrointestinal microbiome at intensive care unit admission and risk for subsequent death or infection. *Intensive Care Med.* **44**, 1203–1211 (2018).
19. Bidell, M. R., Hobbs, A. L. V. & Lodise, T. P. Gut microbiome health and dysbiosis: A clinical primer. *Pharmacother. J. Hum. Pharmacol. Drug Ther.* **42**, 849–857 (2022).
20. Le Guern, R. et al. Colonization resistance against multi-drug-resistant bacteria: A narrative review. *J. Hosp. Infect.* **118**, 48–58 (2021).
21. Lawley, T. D. & Walker, A. W. Intestinal colonization resistance. *Immunology* **138**, 1–11 (2013).
22. Chanderraj, R. et al. In critically ill patients, anti-anaerobic antibiotics increase risk of adverse clinical outcomes. *Eur. Respir J.* **61** (2), 2200910 (2023).
23. Shade, A. et al. Fundamentals of microbial community resistance and resilience. *Front. Microbiol.* **3**, 417 (2012).
24. Moron, R. et al. The importance of the Microbiome in critically ill patients: Role of Nutrition. *Nutrients* **11**, 3002 (2019).
25. Faust, K. et al. Microbial co-occurrence relationships in the human microbiome. *PLoS Comput. Biol.* **8** (7), e1002606 (2012).
26. Currie, K. et al. The acceptability of screening for carbapenemase producing enterobacteriaceae (CPE): Cross-sectional survey of nursing staff and the general publics' perceptions. *Antimicrob. Resist. Infect. Control* **7**, 144 (2018).
27. Radhakrishnan, S. T. et al. Rectal swabs as a viable alternative to faecal sampling for the analysis of gut microbiota functionality and composition. *Sci. Rep.* **13**, 493 (2023).
28. Budding, A. E. et al. Rectal swabs for analysis of the intestinal microbiota. *PLOS One* **9**, e101344 (2014).
29. Reyman, M., van Houten, M. A., Arp, K., Sanders, E. A. M. & Bogaert, D. Rectal swabs are a reliable proxy for faecal samples in infant gut microbiota research based on 16S-rRNA sequencing. *Sci. Rep.* **9**, 16072 (2019).
30. Sharma, N., Bhatia, S., Sodhi, A. S. & Batra, N. Oral microbiome and health. *AIMS Microbiol.* **4**, 42–66 (2018).
31. Ingendoh-Tsakmakidis, A., Eberhard, J., Falk, C. S., Stiesch, M. & Winkel, A. In vitro effects of streptococcus oralis biofilm on peri-implant soft tissue cells. *Cells* **9**, 1226 (2020).
32. Aardema, H. et al. Marked changes in gut microbiota in cardio-surgical intensive care patients: A longitudinal cohort study. *Front. Cell. Infect. Microbiol.* **9**, (2020).
33. McDonald, D. et al. Extreme dysbiosis of the microbiome in critical illness. *mSphere* **1**, 101128msphere00199–101128msphere00116 (2016).
34. Yeh, A. et al. Dysbiosis across multiple body sites in critically ill adult surgical patients. *Shock* **46**, 649 (2016).
35. Kelly, B. J. et al. Composition and dynamics of the respiratory tract microbiome in intubated patients. *Microbiome* **4**, 7 (2016).
36. Zaborin, A. et al. Membership and behavior of ultra-low-diversity pathogen communities present in the gut of humans during prolonged critical illness. *mBio* **5** https://doi.org/10.1128/mbio.01361-14 (2014).
37. Choi, Y. H. et al. Oral microbiota change in intubated patients under mechanical ventilation. *J. Bacteriol. Virol.* **51**, 163–171 (2021).
38. Kitsios, G. D. et al. Respiratory tract dysbiosis is associated with worse outcomes in mechanically ventilated patients. *Am. J. Respir Crit. Care Med.* **202**, 1666–1677 (2020).
39. Agudelo-Ochoa, G. M. et al. Gut microbiota profiles in critically ill patients, potential biomarkers and risk variables for sepsis. *Gut Microbes* **12**, 1707610 (2020).
40. Chopyk, J. et al. Temporal variations in bacterial community diversity and composition throughout intensive care unit renovations. *Microbiome* **8**, 86 (2020).
41. Zafar, H. & Saier, M. H. Gut bacteroides species in health and disease. *Gut Microbes* **13**, 1–20 (2021).
42. Wexler, H. M. Bacteroides: The good, the bad, and the nitty-gritty. *Clin. Microbiol. Rev.* **20**, 593–621 (2007).
43. Krawczyk, B., Wityk, P., Gałęcka, M. & Michalik, M. The many faces of Enterococcus spp.—Commensal, probiotic and opportunistic pathogen. *Microorganisms* **9**, 1900 (2021).
44. Fiore, E., Van Tyne, D. & Gilmore, M. S. Pathogenicity of enterococci. *Microbiol. Spectr.* **7** (4). https://doi.org/10.1128/microbiolspec.GPP3-0053-2018 (2019).
45. Tett, A., Pasolli, E., Masetti, G., Ercolini, D. & Segata, N. Prevotella diversity, niches and interactions with the human host. *Nat. Rev. Microbiol.* **19**, 585–599 (2021).
46. Könönen, E. & Gursoy, U. K. Oral Prevotella species and their connection to events of clinical relevance in gastrointestinal and respiratory tracts. *Front. Microbiol.* **12**, 798763 (2021).
47. Könönen, E., Conrads, G. & Nagy, E. Bacteroides Porphyromonas, Prevotella, Fusobacterium, and Other Anaerobic Gram-negative Rods. *Manual of Clinical Microbiology* 967–993 (John Wiley & Sons, Ltd, 2015). https://doi.org/10.1128/9781555817381.ch54
48. Eribe, E. R. K. & Olsen, I. Leptotrichia species in human infections II. *J. Oral Microbiol.* **9** (1), 1368848 (2017).

49. Tsuzukibashi, O. et al. Isolation and identification methods of Rothia species in oral cavities. *J. Microbiol. Methods* **134**, 21–26 (2017).
50. Yu, M. et al. Characterization of cytotoxic Citrobacter braakii isolated from human stomach. *FEBS Open. Bio* **14**, 487–497 (2024).
51. Lurgi, M., Thomas, T., Wemheuer, B., Webster, N. S. & Montoya, J. M. Modularity and predicted functions of the global sponge-microbiome network. *Nat. Commun.* **10**, 992 (2019).
52. Liu, Y. et al. Microbial Community structure and ecological networks during simulation of diatom sinking. *Microorganisms* **10**, 639 (2022).
53. Feit, B., Blüthgen, N., Traugott, M. & Jonsson, M. Resilience of ecosystem processes: A new approach shows that functional redundancy of biological control services is reduced by landscape simplification. *Ecol. Lett.* **22**, 1568–1577 (2019).
54. Akavipat, P., Thinkhamrop, J., Thinkhamrop, B. & Sriraj, W. Acute physiology and chronic health evaluation (APACHE) II score – The clinical predictor in neurosurgical intensive care unit. *Acta Clin. Croat.* **58**, 50–56 (2019).
55. Mumtaz, H. et al. APACHE scoring as an indicator of mortality rate in ICU patients: A cohort study. *Ann. Med. Surg.* **85**, 416–421 (2023).
56. Tamames, J. & Puente-Sánchez, F. SqueezeMeta, a highly portable, fully automatic metagenomic analysis pipeline. *Front. Microbiol.* **9**, 3349 (2019).
57. Tamames, J. et al. SqueezeMeta [software]. (accessed 16 Oct 2024). https://github.com/jtamames/SqueezeMeta.
58. Bolger, A. M. et al. Trimmomatic [software]. ((accessed 16 Oct 2024). https://github.com/usadellab/Trimmomatic.
59. Buchfink, B., Xie, C. & Huson, D. H. Fast and sensitive protein alignment using DIAMOND. *Nat. Methods* **12**, 59–60 (2015).
60. Buchfink, B. et al. DIAMOND [software]. (accessed 16 Oct 2024). https://github.com/bbuchfink/diamond.
61. Sayers, E. W. et al. GenBank 2023 update. *Nucleic Acids Res.* **51**, D141–D144 (2023).
62. McMurdie, P. J. & Holmes, S. Phyloseq: An R package for reproducible interactive analysis and graphics of microbiome census data. *PloS One* **8**, e61217 (2013).
63. McMurdie, P. J. et al. Phyloseq [software]. (accessed 16 Oct 2024). https://github.com/joey711/phyloseq.
64. Oksanen, J. et al. Vegan [software]. (accessed 16 Oct 2024). https://github.com/vegandevs/vegan.
65. Wickham, H. et al. ggplot2: Create Elegant Data Visualisations Using the Grammar of Graphics. (2024).
66. Wickham, H. et al. ggplot2 [software]. (accessed 16 Oct 2024). https://github.com/tidyverse/ggplot2.
67. Peschel, S., Müller, C. L., von Mutius, E., Boulesteix, A. L. & Depner, M. NetCoMi: Network construction and comparison for microbiome data in R. *Brief. Bioinform.* **22**, bbaa290 (2021).
68. Peschel, S. et al. NetCoMi [software]. (accessed 16 Oct 2024). https://github.com/stefpeschel/NetCoMi.
69. Gu, Z., Gu, L., Eils, R., Schlesner, M. & Brors, B. Circlize implements and enhances circular visualization in R. *Bioinformatics* **30**, 2811–2812 (2014).
70. Gu, Z. et al. Circlize [software]. (accessed 16 Oct 2024). https://github.com/jokergoo/circlize.
71. Richards, T., Stephen, J. & Lui, C. L. Severe disseminated Veillonella parvula infection including endocarditis, bilateral psoas abscess, discitis, and osteomyelitis but sparing spinal and hip prostheses: A case report. *J. Med. Case Rep.* **16**, 157 (2022).
72. Holt, S. C. & Ebersole, J. L. Porphyromonas gingivalis, Treponema denticola, and Tannerella forsythia: The 'red complex', a prototype polybacterial pathogenic consortium in periodontitis. *Periodontol. 2000* **38**, 72–122 (2005).
73. Cunningham, M. W. Pathogenesis of group a streptococcal infections. *Clin. Microbiol. Rev.* **13**, 470–511 (2000).
74. Scholte, J. B. J. et al. Empirical antibiotic therapy for pneumonia in intensive care units: A multicentre, retrospective analysis of potentially pathogenic microorganisms identified by endotracheal aspirates cultures. *Eur. J. Clin. Microbiol. Infect. Dis. Off. Publ. Eur. Soc. Clin. Microbiol.* **34**, 2295–2305 (2015).
75. Krzyściak, W., Jurczak, A., Kościelniak, D., Bystrowska, B. & Skalniak, A. The virulence of Streptococcus mutans and the ability to form biofilms. *Eur. J. Clin. Microbiol. Infect. Dis. Off. Publ. Eur. Soc. Clin. Microbiol.* **33**, 499–515 (2014).
76. Schwab, F., Geffers, C., Behnke, M. & Gastmeier, P. ICU mortality following ICU-acquired primary bloodstream infections according to the type of pathogen: A prospective cohort study in 937 Germany ICUs (2006–2015). *PloS One* **13**, e0194210 (2018).
77. Szczuka, E., Krzymińska, S., Bogucka, N. & Kaznowski, A. Multifactorial mechanisms of the pathogenesis of methicillin-resistant Staphylococcus hominis isolated from bloodstream infections. *Antonie Van Leeuwenhoek* **111**, 1259–1265 (2018).
78. Otto, M. Staphylococcus epidermidis pathogenesis. *Methods Mol. Biol. Clifton NJ* **1106**, 17–31 (2014).
79. Cameron, D. R. et al. Insights on virulence from the complete genome of Staphylococcus capitis. *Front. Microbiol.* **6**, 980 (2015).
80. Ohl, M. et al. Hospital privacy curtains are frequently and rapidly contaminated with potentially pathogenic bacteria. *Am. J. Infect. Control* **40**, 904–906 (2012).
81. Hawkes, C. G. et al. Selenomonas sputigena interactions with Gingival epithelial cells that promote inflammation. *Infect. Immun.* **91**, e0031922 (2023).
82. Jajere, S. M. A review of Salmonella enterica with particular focus on the pathogenicity and virulence factors, host specificity and antimicrobial resistance including multidrug resistance. *Vet. World* **12**, 504–521 (2019).
83. Qin, S. et al. Pseudomonas aeruginosa: Pathogenesis, virulence factors, antibiotic resistance, interaction with host, technology advances and emerging therapeutics. *Signal. Transduct. Target. Ther.* **7**, 1–27 (2022).
84. Armbruster, C. E., Mobley, H. L. T. & Pearson, M. M. Pathogenesis of Proteus mirabilis infection. *EcoSal Plus* **8** https://doi.org/10.1128/ecosalplus.ESP-0009-2017 (2018).
85. Hafström, C. & Dahlén, G. Pathogenicity of Prevotella intermedia and Prevotella nigrescens isolates in a wound chamber model in rabbits. *Oral Microbiol. Immunol.* **12**, 148–154 (1997).
86. Müller-Schulte, E., Heimann, K. C. & Treder, W. Peptoniphilus asaccharolyticus - commensal, pathogen or synergist? Two case reports on invasive Peptoniphilus asaccharolyticus infection. *Anaerobe* **59**, 159–162 (2019).
87. Quillin, S. J. & Seifert, H. S. Neisseria gonorrhoeae host-adaptation and pathogenesis. *Nat. Rev. Microbiol.* **16**, 226–240 (2018).
88. Liu, H., Zhu, J., Hu, Q. & Rao, X. Morganella morganii, a non-negligent opportunistic pathogen. *Int. J. Infect. Dis. IJID off. Publ. Int. Soc. Infect. Dis.* **50**, 10–17 (2016).
89. de Vries, S. P. W., Bootsma, H. J., Hays, J. P. & Hermans, P. W. Molecular aspects of Moraxella catarrhalis Pathogenesis. *Microbiol. Mol. Biol. Rev. MMBR* **73**, 389–406 (2009).
90. Abbas, R. et al. General overview of Klebsiella pneumonia: Epidemiology and the role of siderophores in its pathogenicity. *Biology* **13**, 78 (2024).
91. Darby, A. et al. Cytotoxic and pathogenic properties of Klebsiella oxytoca isolated from Laboratory animals. *PloS One* **9**, e100542 (2014).
92. Mittal, J., Ponce, M. G., Gendlina, I. & Nosanchuk, J. D. Histoplasma Capsulatum: Mechanisms for pathogenesis. *Curr. Top. Microbiol. Immunol.* **422**, 157–191 (2019).
93. Han, Y. W. Fusobacterium nucleatum: A commensal-turned pathogen. *Curr. Opin. Microbiol.* **0**, 141–147 (2015).
94. Kaper, J. B., Nataro, J. P. & Mobley, H. L. T. Pathogenic Escherichia coli. *Nat. Rev. Microbiol.* **2**, 123–140 (2004).
95. Fiore, E., Van Tyne, D. & Gilmore, M. S. Pathogenicity of enterococci. *Microbiol. Spectr.* **7**. https://doi.org/10.1128/microbiolspec.gpp3-0053-2018
96. Salimiyan Rizi, K., Ghazvini, K. & Farsiani, H. Clinical and pathogenesis overview of Enterobacter infections. *Rev. Clin. Med.* **6**, 146–154 (2020).
97. Suwanagool, S., Rothkopf, M. M., Smith, S. M., LeBlanc, D. & Eng, R. Pathogenicity of Eikenella corrodens in humans. *Arch. Intern. Med.* **143**, 2265–2268 (1983).
98. Zaragoza, O. Basic principles of the virulence of Cryptococcus. *Virulence* **10**, 490–501 (2019).

99. Jamal, S. B. et al. Pathogenesis of Corynebacterium diphtheriae and available vaccines: An overview. *Glob. J. Infect. Dis. Clin. Res.* **3**, 020–024 (2017).
100. Mayer, F. L., Wilson, D. & Hube, B. Candida albicans pathogenicity mechanisms. *Virulence* **4**, 119 (2013).
101. Arce, R. M. et al. Characterization of the invasive and inflammatory traits of oral Campylobacter rectus in a murine model of fetoplacental growth restriction and in trophoblast cultures. *J. Reprod. Immunol.* **84**, 145–153 (2010).
102. Paulussen, C. et al. Ecology of aspergillosis: Insights into the pathogenic potency of aspergillus fumigatus and some other aspergillus species. *Microb. Biotechnol.* **10**, 296–322 (2017).
103. Dagenais, T. R. T. & Keller, N. P. Pathogenesis of aspergillus fumigatus in invasive aspergillosis. *Clin. Microbiol. Rev.* **22**, 447–465 (2009).
104. Talapko, J. et al. Aggregatibacter actinomycetemcomitans: From the oral cavity to the heart valves. *Microorganisms* **12**, 1451 (2024).
105. Gajdács, M. & Urbán, E. The pathogenic role of Actinomyces spp. and related organisms in Genitourinary infections: Discoveries in the New, Modern Diagnostic Era. *Antibiot. Basel Switz.* **9**, 524 (2020).
106. d'Enfert, C. Hidden killers: Persistence of opportunistic fungal pathogens in the human host. *Curr. Opin. Microbiol.* **12**, 358–364 (2009).
107. Jasemi, S. et al. Antibiotic resistance pattern of Bacteroides fragilis isolated from clinical and colorectal specimens. *Ann. Clin. Microbiol. Antimicrob.* **20**, 27 (2021).
108. Mishra, S. & Imlay, J. A. An anaerobic bacterium, Bacteroides thetaiotaomicron, uses a consortium of enzymes to scavenge hydrogen peroxide. *Mol. Microbiol.* **90**. https://doi.org/10.1111/mmi.12438 (2013).
109. Dhanashree, Rajashekharan, S., Krishnaswamy, B. & Kammara, R. Bifid shape is intrinsic to Bifidobacterium adolescentis. *Front. Microbiol.* **8**, 478 (2017).
110. Liu, X. et al. Blautia—A new functional genus with potential probiotic properties? *Gut Microbes* **13**, 1875796 .
111. Shibata, M. et al. Mouse model of anti-obesity effects of Blautia hansenii on diet-induced obesity. *Curr. Issues Mol. Biol.* **45**, 7147–7160 (2023).
112. Jabeen, I., Islam, S., Hassan, A. K. M. I., Tasnim, Z. & Shuvo, S. R. A brief insight into Citrobacter species - A growing threat to public health. *Front. Antibiot.* **2**, (2023).
113. Wells, C. L. & Wilkins, T. D. Clostridia Sporeforming Anaerobic Bacilli. in*Medical Microbiology*. (eds Baron, S.) (University of Texas Medical Branch at Galveston, 1996).
114. Cassir, N., Benamar, S. & La Scola, B. Clostridium butyricum: From beneficial to a new emerging pathogen. *Clin. Microbiol. Infect. Off. Publ. Eur. Soc. Clin. Microbiol. Infect. Dis.* **22**, 37–45 (2016).
115. Edwards, A. N., Suárez, J. M. & McBride, S. M. Culturing and maintaining Clostridium difficile in an anaerobic environment. *J. Vis. Exp. JoVE* 50787. https://doi.org/10.3791/50787 (2013).
116. Dróżdż, M., Makuch, S., Cieniuch, G., Woźniak, M. & Ziółkowski, P. Obligate and facultative anaerobic bacteria in targeted cancer therapy: Current strategies and clinical applications. *Life Sci.* **261**, 118296 (2020).
117. Said, M. S., Tirthani, E. & Lesho, E. Enterococcus Infections. in *StatPearls* (StatPearls Publishing, 2024).
118. Mukherjee, A., Lordan, C., Ross, R. P. & Cotter, P. D. Gut microbes from the phylogenetically diverse genus Eubacterium and their various contributions to gut health. *Gut Microbes* **12**, 1802866 (2020).
119. Wang, Y. et al. Eubacterium rectale contributes to colorectal cancer initiation via promoting colitis. *Gut Pathog.* **13**, 2 (2021).
120. Khan, M. T. et al. Synergy and oxygen adaptation for development of next-generation probiotics. *Nature* **620**, 381–385 (2023).
121. Lee, S. J. et al. Increasing Fusobacterium infections with Fusobacterium varium, an emerging pathogen. *PloS One* **17**, e0266610 (2022).
122. Roberts, B. N., Chakravarty, D., Gardner, J. C., Ricke, S. C. & Donaldson, J. R. Listeria monocytogenes response to anaerobic environments. *Pathogens* **9**, 210 (2020).
123. Giannella, R. A. Salmonella. in *Medical Microbiology* (ed. Baron, S.) (University of Texas Medical Branch at Galveston, Galveston (TX, 1996).
124. Zhang, T., Li, Q., Cheng, L., Buch, H. & Zhang, F. Akkermansia muciniphila is a promising probiotic. *Microb. Biotechnol.* **12**, 1109–1125 (2019).
125. Ezeji, J. C. et al. Parabacteroides distasonis: Intriguing aerotolerant gut anaerobe with emerging antimicrobial resistance and pathogenic and probiotic roles in human health. *Gut Microbes* **13**, 1922241 .
126. Turroni, F. et al. Bifidobacterium bifidum: A key member of the early human gut microbiota. *Microorganisms* **7** (2019).
127. Mills, S., Yang, B., Smith, G. J., Stanton, C. & Ross, R. P. Efficacy of Bifidobacterium longum alone or in multi-strain probiotic formulations during early life and beyond. *Gut Microbes* **15**, 2186098 .
128. Hiippala, K., Kainulainen, V., Kalliomäki, M., Arkkila, P. & Satokari, R. Mucosal prevalence and interactions with the Epithelium Indicate Commensalism of Sutterella spp. *Front. Microbiol.* **7**, 1706 (2016).

Author contributions

A.P. and P.N. were responsible for the collection, registration, and interpretation of patient samples and clinical data. P.F. coordinated the bioinformatic analyses and assisted in preparing the figures. A.SZ.R., M.M., E.SZ.T., D.P., and T.P. processed biological samples, extracted nucleic acids, conducted shotgun sequencing, and performed statistical analyses and figure preparation. A.S., F.G., K.G., and R.S. participated in the interpretation of the data. L.S., S.B., and J.R. contributed to the conceptual framework and critically revised the manuscript for key intellectual content. M.P. led the conceptualization, guided the analyses, interpreted data, and was the principal author of the manuscript. All authors reviewed the manuscript.

Declarations

Competing interests

The authors declare no competing interests.

Additional information

Supplementary Information The online version contains supplementary material available at https://doi.org/10.1038/s41598-024-78102-1.

Correspondence and requests for materials should be addressed to M.P.

Reprints and permissions information is available at www.nature.com/reprints.